ChemPubSoc Europe

DOI: 10.1002/cctc.201800523

CHEMCATCHEM Full Papers

Competitive Adsorption of Nitrite and Hydrogen on Palladium during Nitrite Hydrogenation

Rolf Sybren Postma,[a] Roger Brunet Espinosa,[a, b] and Leon Lefferts*[a]

Nitrite hydrogenation is studied in steady-state as well as transient operation using a Pd catalyst in a tubular membrane contactor reactor. A negative reaction order in hydrogen in steady state operation proofs that hydrogen and nitrite adsorb competitively. In transient operation, feeding nitrite to the Pd surface fully covered with hydrogen results initially in very low conversion of nitrite, speeding up once hydrogen is removed from part of the Pd surface. Additional proof for competitive adsorption between hydrogen and nitrite is provided by the observation that exposure of a nitrite-covered catalyst to hydrogen induces desorption of nitrite. Formation of ammonia in these experiments proceeds via two pathways, first via a fast reaction followed by extremely slow hydrogenation of adsorbed N atoms, which is kinetically not relevant. This information is relevant for designing effective and selective catalysts when operating at very low nitrite concentration.

Introduction

The concentration of nitrate in surface and ground water reservoirs has been steadily increasing over the last decades caused by increasing human population and intensified agriculture.[1] Exposure to nitrate has been correlated with various adverse health effects, such as blue baby syndrome and intestinal cancer. Furthermore, it can lead to eutrophication in water reservoirs.[2–4] For these reasons the European Union has limited the concentration of nitrate (NO_3^--N) in drinking water to 50 mg/l and legislation in the United States is even more strict with 10 mg/l.[5,6] Common methods to remove nitrite (NO_2^-) and nitrate include reverse osmosis, electro-dialysis, ion exchange and biological degradation.[7–9] Biological degradation is generally not possible for drinking water because of the absence of nutrients for sustaining bacterial growth. The other methods have the drawbacks that nitrate rich waste streams are produced which cannot be simply disposed and the need to convert nitrate and nitrite remains. Therefore, catalytic hydrogenation of nitrates to nitrogen is a promising technique.[8–10] This method uses noble-metal catalysts such as palladium or platinum in combination with a promotor, most commonly copper, to reduce nitrate to nitrogen. High selectivity is required because of the formation of ammonia as a non-desired by product.[11,12] Despite significant research,[13–15] the issue of preventing formation of ammonia is not yet resolved, especially when using practical continuous operated reactors.[15] Both reaction rate and selectivity depend greatly on the hydrogen concentration at the catalyst surface. A high hydrogen concentration leads at one hand to fast conversion, but at the other hand also to low selectivity to N_2.[16]

Nitrate hydrogenation proceeds via two consecutive reactions. First nitrate (NO_3^-) is converted to nitrite (NO_2^-), requiring a bi-metallic catalyst (e.g. Pd–Cu). The second reaction step is catalyzed by a mono-metallic noble catalyst, generally palladium. In this step nitrite is hydrogenated to either nitrogen or ammonia in a very fast reaction. The key in this second step is to maintain a high reaction rate to attain complete conversion, without inducing high selectivity to ammonia.[17,18]

Catalytic membrane reactors have been studied for nitrite and nitrate hydrogenation[19–25] as such intensified reactors allow not only smaller reactor sizes and lower energy consumption,[26] but also can improve the control on local concentrations at the active site. Brunet-Espinosa et al.[27,28] demonstrated that a small tubular membrane contactor reactor (internal radius 0.9 mm) allows combining high conversion with high selectivity to N_2 by dosing a small amount of hydrogen all along the reactor length (Figure 1). The tube wall consisted of macro-porous α-alumina, in which carbon nanofibers are grown, acting as support for the palladium particles. The outside surface of the tube is covered with a PDMS layer to

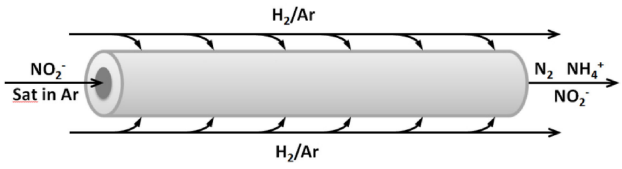

Figure 1. Schematic over and flow operation of the membrane reactor [27]

[a] R. S. Postma, Dr. R. Brunet Espinosa, Prof. Dr. L. Lefferts
Catalytic Processes and Materials group
Faculty of Science and Technology
MESA + Institute for Nanotechnology
University of Twente
PO Box 217, 7500 AE Enschede (The Netherlands)
E-mail: l.lefferts@utwente.nl
[b] Dr. R. Brunet Espinosa
Present address:
Beele Engineering
Beunkdijk 11, 7122 NZ Aalten (The Netherlands)

make it impermeable to water, while allowing gas (H_2) transport via diffusion.

It was demonstrated that this reactor design indeed results in high selectivity to N_2 at high conversion.[22] It was also reported that, depending on the distribution of CNFs and Pd through the α-alumina wall, the reaction rate can be suppressed by increasing the hydrogen pressure.[28] This result suggests a negative reaction order in H_2, indicative for competitive adsorption of NO_2^- and H_2, which is clearly not in agreement with kinetic data on nitrite and nitrate hydrogenation reported so far. Experiments in conventional slurry and fixed bed reactors resulted in reaction orders in nitrite varying between 1 and 0.7, whereas the reaction order in hydrogen is in the window between 0 and 0.3.[29–31] It was argued that the apparent negative reaction order may be caused by the extreme broad window of the ratios of the NO_2^- and H_2 concentrations encountered at different positions in the membrane contactor reactor. The reader is referred to [28] for further details.

The goal of this paper is to test the hypothesis of competitive adsorption of H_2 and NO_2^- on Pd by varying the nitrite concentration in steady-state experiments as well as by using transient experiments in with the membrane contactor reactor.

Results

Steady State Operation

The results shown in Figure 2a are adapted from [28], showing the effect of changing the hydrogen partial pressure outside the membrane on nitrite conversion. Figure 2b and 2c show similar results measured at higher NO_2^- concentration. The result show that the selectivity is shifting towards ammonia, as expected, with increasing H_2 concentration in the gas mixture. In addition, increasing hydrogen concentration causes the conversion to decrease at all three nitrite concentrations. The effect is partly suppressed though by increasing the NO_2^- concentration.

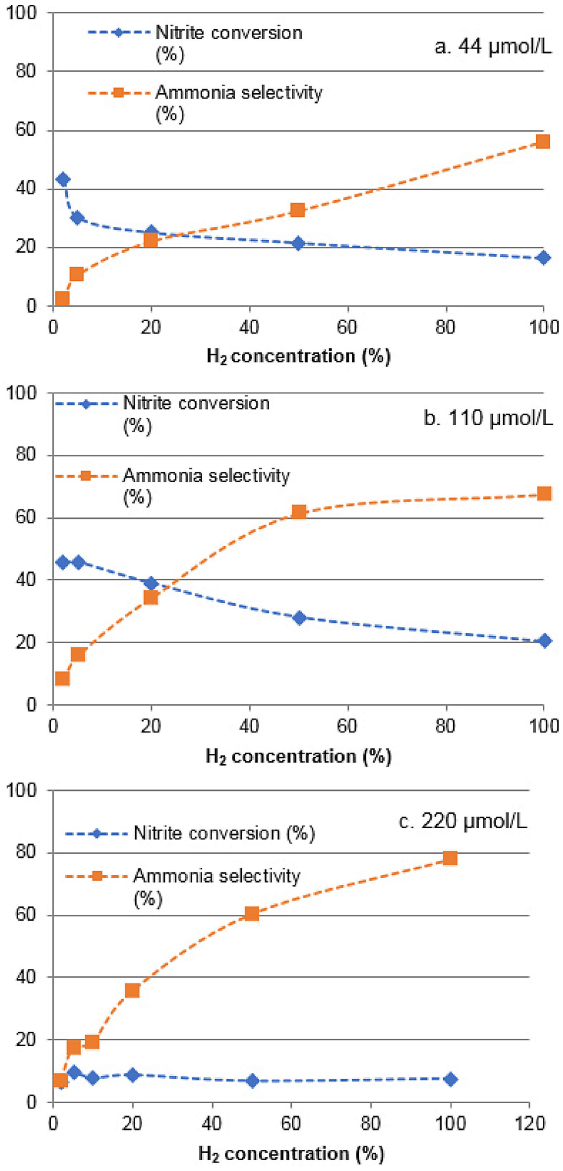

Figure 2. Effect of hydrogen concentration at the outside of the membrane contactor (balanced with Ar at 1 atm) on nitrite conversion and selectivity in the membrane reactor operated with a liquid flow rate of 0.05 ml/min at room temperature. Experiments were performed with different nitrite concentrations: a. 44 µmol/L; b. 110 µmol/L; c. 220 µmol/L.

Transient Operation

Figure 3 shows the transient response on feeding a nitrite solution to the reactor to a fully hydrogen saturated Pd catalyst. The start of the experiment (time is zero) is defined as the moment just before the nitrite and ammonia concentration start to increase. The actual switch was made 50 minutes earlier, the delay being caused by the residence time between the pump and the sample-port of the IC. Figure 3a shows an oscillation in the nitrite concentration at the beginning of the experiment, after which nitrite slowly increases up to the concentration in the feed. Figure 3b zooms in on the first 20 h of the experiment, providing more details of the oscillation in the nitrite concentration. Ammonia forms only initially, quickly dropping to zero. Figure 3c presents a further zoom in on the first 4 hours of the experiment, together with the result of two blank experiments showing the nitrite responses with an empty reactor and a catalyst without any adsorbed hydrogen. Figure 3d shows the profiles of nitrite conversion and selectivity to ammonia, calculated from Figure 3b.

Both blank experiments in Figure 3c give a similar result that is clearly different from the transient nitrite concentration profile in the experiment, allowing an estimation of the amount of NO_2^- that is converted based on the nitrite profiles in Figure 3a, b and c. Initially, the nitrite conversion is significant as the breakthrough of NO_2^- is significantly delayed (Figure 3c) and $9.2 \cdot 10^{-2}$ µmol nitrite is converted, until the moment the first local maximal concentration is reached after 2 hours. After that, the nitrite concentration first reaches a minimum,

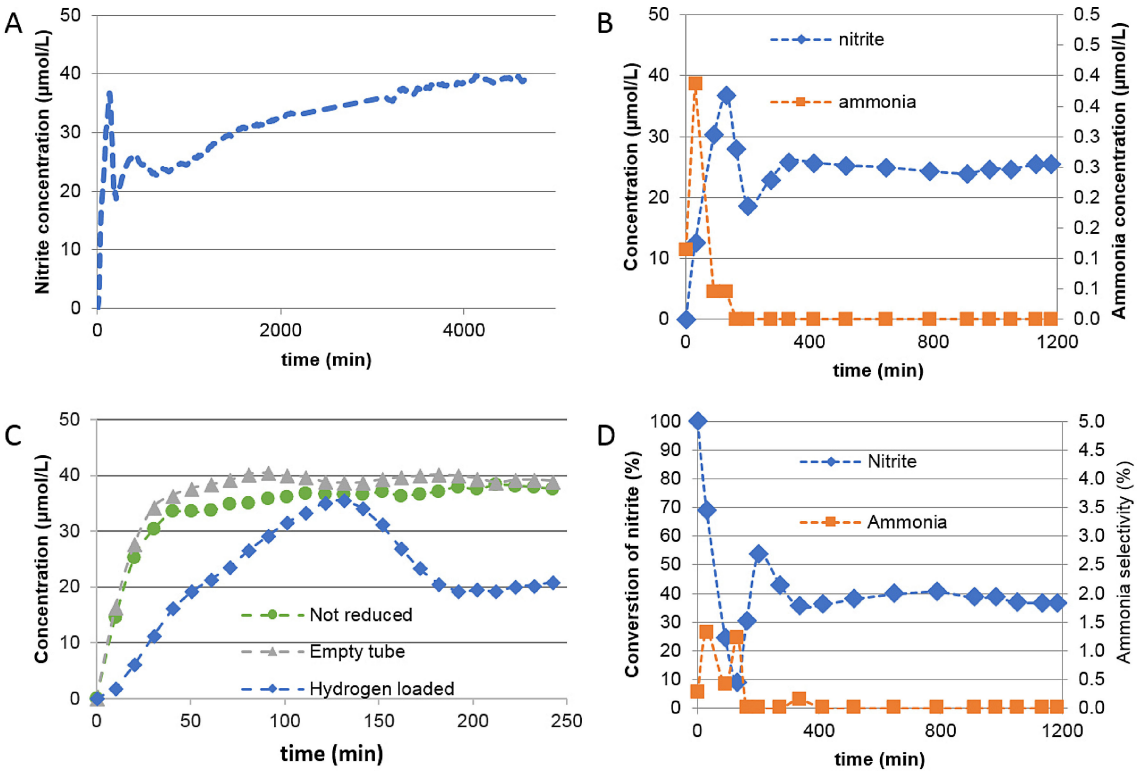

Figure 3. Transient response on feeding a nitrite solution to the hydrogen saturated membrane reactor. Experiments were performed at room temperature with 40 µmol/L nitrite solution and liquid flow rate of 0.05 ml/min. a) The nitrite concentration curve during the full experiment; b) The nitrite and ammonia concentration curve at the beginning of the experiment; c) presents the nitrite response for two blank experiments together with the nitrite response in figure b, i.e. first, the reactor is replaced with an empty tube with identical dimensions and second, the reactor is not treated with hydrogen; d) conversion and selectivity curve based on graph c.

converting an additional $2.7 \cdot 10^{-2}$ µmol, where after a second local maximum is observed (converting an additional 0.12 µmol). Finally, it takes typically 60 h before conversion of nitrite stops, indicating exhaustion of hydrogen in the system as will be discussed in more detail later. The total quantity of consumed nitrite in the 60 h experiment (Figure 3a) is 1.9 µmol and the total amount of formed ammonia is $9.3 \cdot 10^{-4}$ µmol, calculated from Figure 3b.

Figure 4 presents the transient response on feeding 1 bar of hydrogen at the shell side and flowing milli-q water through the inside, directly after the experiment in Figure 3, showing desorption of nitrite and ammonia. The concentration of the nitrite flushed reaches nearly twofold (76 µmol/L) the feed concentration used during nitrite adsorption (40 µmol/L), indicating that the presence of H_2 induces desorption of nitrite. It should be noted that the absolute value of the maximum is not well reproducible but the increase in concentration is; this is caused by the fact that the frequency of sampling of the IC is limited so that the actual value of the maximum renders inaccurate. The ammonia concentration reaches a maximum concentration of 130 µmol/L a little bit later. Figure 4b compares the nitrite concentration gradient, identical to Figure 4a, with two blank experiments; i.e. with an empty tube and with a catalyst that was initially hydrogen free (as in Figure 3c). The 50 min delay in the blank experiments in Figure 4b is caused by the residence time in the system between the pump and the sample point of the IC. Changing the gas-phase in the reactor shell is almost instantaneous in contrast to changing the liquid in the reactor tube. Most of the delay is caused by the volume of the pump and of a filter that is mounted between the reactor and the IC, protecting the IC against e.g. CNFs. The ammonia and nitrite responses are about 10 minutes faster than the nitrite breakthrough in the blank experiments (Figure 4a & 4b).

It appears that the H_2-free catalyst desorbed a small amount of nitrite, resulting in a small plateau in the nitrite profile compared to the empty reactor. Therefore, the amount of nitrite desorbed during the experiment (Figure 4a) is calculated based on the blank with the empty reactor, resulting $8.9 \cdot 10^{-2}$ µmol. In any case, the amount of nitrite desorbing is very much lower when the catalyst was not reduced before NO_2^- was adsorbed. The amount of ammonia released during the first two hours (Figure 4a) amounts to $1.6 \cdot 10^{-1}$ µmol. However, the formation of ammonia continues at a very low rate as can be seen in Figure 4c, as a low concentration of ammonia is observed during 65 h. The total amount of ammonia formed is 0.3 µmol of ammonia.

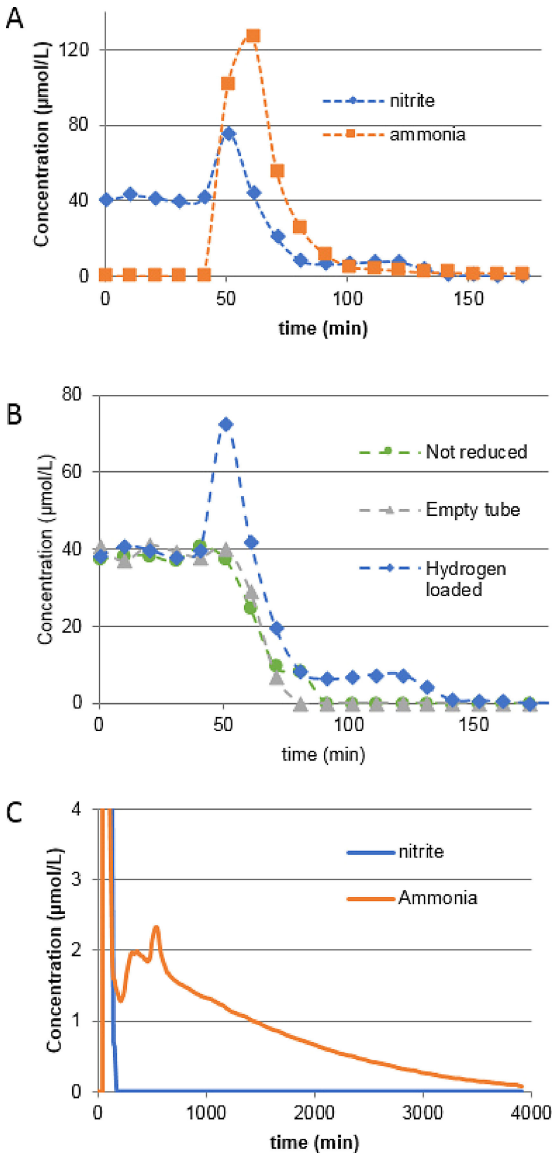

Figure 4. Transient response when feeding H_2 to the shell of the membrane reactor after the experiment reported in Figure 3. Experiments were performed using degassed milli-q water with a liquid flow rate of 0.05 ml/min at room temperature. a) The first 150 minutes of the experiment; b) nitrite concentration profile identical to figure a compared to blank experiments with an empty tube and with a reactor not treated with H_2; c) The full experiment, zoomed in along the y-axis

Discussion

Steady State Operation

The trends in conversion with hydrogen partial pressure in Figure 2 confirms that the reaction can be suppressed by hydrogen, resulting in an apparent negative reaction order in H_2. As discussed in [22], this suggests competitive adsorption between nitrite and hydrogen assuming a Langmuir-Hinshelwood mechanism. The observation in Figures 2b and 2c demonstrate that this effect becomes weaker at higher NO_2^- concentrations, consistent with the assumption of competitive adsorption of H_2 and nitrite.

Transient Operation

The total quantity of nitrite consumed (1.9 µmol) and ammonia formed ($9.3 \cdot 10^{-4}$ µmol) during exposure to nitrite in Figure 3a and 3b, can be related to the amount of hydrogen available in and on the catalyst. Overnight treatment in 1 bar H_2 results in the formation of palladium hydride ($PdH_{0.7}$).[32,33] Based on the amount of Pd in the reactor it can be calculated that 3.48 µmol H is available. Furthermore, we assume the presence of a monolayer of hydrogen at the surface of the Pd-hydride; it can be estimated that this equals to 0.60 µmol H, based on an average Pd particle size of 9 nm. It should be noted that this assumption is necessary to explain the amounts of NH_4^+ produced and NO_2^- converted as observed. Thus, we assume that in total 4.1 µmol atomic hydrogen is available. Considering that conversion of one NO_2^- ion to NH_4^+ consumes 6 H atoms, whereas conversion to N_2 consumes only 3 H atoms, it can be estimated that 1.3 µmol NO_2^- can be converted to products. The remaining 0.6 µmol NO_2^- apparently adsorbs on the catalyst, forming about a monolayer of N-containing species on the catalyst surface. This implies that 1.3 µmol nitrite is indeed converted to N_2 because it is not reasonable to assume that a multilayer of N containing species can form. Interestingly, slowly feeding nitrite to a fully hydrogenated catalyst, causes significant nitrite consumption, but hardly any ammonia is formed. This is not in line with the general observations in steady state experiments where a high H/N ratio in the feed causes high selectivity to ammonia. It may be speculated that this is caused by the presence of Pd β-hydride or absence of free dissolved H_2 in the transient experiment, in contrast to a steady-state experiment.

The break-through curve in Figure 3c allows calculation of the amount of nitrite consumed during the first two hours: i.e. 0.09 µmol. Again, the amount of ammonia formed is two orders of magnitude smaller. Therefore, in this time window nitrite either adsorbs causing a surface coverage of 15%, or is converted to N_2, consuming 0.27 µmol H, or a combination of these two options.

Surprisingly, after 2 hours (Figure 3) nitrite consumption stops almost completely, followed by a rapid acceleration in consumption during the third hour. These effects are assigned to competition between H and nitrite at the Pd surface. H_{ads} first prevents further adsorption or reaction of nitrite, causing the conversion of nitrite to decrease to almost zero after 2 hours. Nevertheless, the slow consumption of adsorbed H is making additional surface sites available for adsorption and conversion of nitrite to N_2, liberating even more adsorption sites and accelerating the reaction rate, as seen in the third hour. In other words, these observations support the hypothesis that adsorption of hydrogen and nitrite compete. On the other hand, it also follows that a relatively small fraction of the H atoms, or a small fraction of surface sites are available to respectively adsorb or convert 0.09 µmol NO_2^- during the first two hours, as discussed above.

The reason for the second, much weaker local maximum in the nitrite concentration (Figure 3) after about 8 hours remains unclear. It may be speculated that this is caused by consump-

tion of roughly a mono-layer of H atoms at that moment in the experiment, but it may also be caused by partial disappearance of β-Pd-hydride in combination with a broad Pd particle size distribution. Additional work would be needed to confirm this.

Ebbesen et al.[34,35] performed similar transient experiments using ATR-IR spectroscopy, reporting very similar results. First, the formation of ammonia is confirmed when nitrite is introduced to a catalyst saturated with hydrogen and second, formation of adsorbed species is observed, assigned to NO_a and $NH_{2,a}$. This agrees well with the overall balance over the experiment during 80 hours. The amount of H present can account for conversion of 1.3 μmol nitrite to N_2; thus, the remaining 0.6 μmol is responsible for formation of NO_a and $NH_{2,a}$. Apparently, the total surface coverage at the end of the experiment is about 1 monolayer (ML). Unfortunately this cannot be confirmed quantitatively with ATR-IR experiments although the intensities reported do indicate significant surface coverage.[34,35] It should be noted that the typical time constant of the experimental results in this work is about 2 orders of magnitude larger compared to the ATR-IR experiments, which is simply caused by a similar difference in the ratio of the amount of nitrite fed per time unit and the amount of Pd surface present in both experiments.

In the second part of the experiment (Figure 4), the adsorbed species are exposed to H_2. The most important observation is that presence of H_2 causes desorption of nitrite, providing direct evidence for competitive adsorption of these species. It can be estimated that about 0.032 (±0.02) μmol NO_2^- desorbed in the window between 40 and 80 minutes, based on the difference with the blank experiment. This equals about 5% of a ML. Remarkably, the desorption is observed earlier than the nitrite flushing out in Figure 4b, which is caused by the fact that changing the gas-phase in the reactor shell is almost instantaneous compared to the response time of the liquid in the tube. In other words, hydrogen is already present while nitrite is not yet flushed out, obtaining strong evidence for competitive adsorption of H_2 and NO_2^-. Next, a plateau is observed until about 140 minutes, desorbing 0.016 μmol nitrite, at the same concentration that is observed for a short time with a reactor that was not pre-treated with H_2. Note that the delay of 40 minutes in Figure 4 is caused by the residence time in tubing and filters between the reactor and IC sample point.

Two domains can be distinguished regarding the formation of ammonia. Fast initial formation of ammonia is probably caused by presence of $NH_{2(ads)}$ species on the catalyst surface. During about 15 minutes before appearance of the NH_4^+ peak, the catalyst is already exposed to hydrogen; it is likely that during this period adsorbed NO_a species are converted to N_2, based on the IR study by Ebbesen et al..[34] The additional delay of 30 minutes before this is caused by the residence time in the equipment between the reactor and the IC sample-valve. After this fast formation of ammonia, ammonia is being formed slowly but continuously during more than 60 hours, as can been seen in Figure 4c. This observation agrees well with result by Zhao et al.,[36] showing strong evidence for the presence of atomic nitrogen (N_{ads}) on the surface as the adsorbed species is not visible with IR spectroscopy. This species is converted to ammonia at a very low pace and therefore it is probably not kinetically relevant. The amount of ammonia formed is about 0.14 μmol, equivalent to 0.25 ML. The small variation in ammonia concentration between 200 and 700 minutes in Figure 4C, involving a tiny amount of ammonia, is not yet understood.

In summary the following reaction scheme is proposed. Starting from Pd fully saturated with hydrogen, nitrite first cannot adsorb resulting in very low conversion, except for rapid formation of a very small amount of ammonia. Partial removal of hydrogen accelerates nitrite hydrogenation, forming nitrogen exclusively. When hydrogen on the Pd is starting to deplete, nitrous species are trapped on the Pd surface in various forms, $NH_{x,ads}$, $NO_{x,ads}$ and N_{ads}. Exposure of the catalyst to hydrogen and nitrite-free water induces desorption of NO_2^-, but also hydrogenation of the surface species. Based on previous work we propose that $NO_{x,ads}$ reacts relatively fast to N_2, whereafter $NH_{x,ads}$ converts to NH_4^+. Finally, very slow hydrogenation of N to NH_4^+ is confirmed in this work.

The notice of competitive adsorption of nitrite and H_2 is important for designing catalytic processes for removing nitrate and nitrite from drinking water, as concentrations of such contaminants is usually rather low and, more importantly, need to be removed to increasingly stricter and lower levels. Therefore, the hydrogen concentration is preferably low in the part of the reactor with low nitrate/nitrite concentration, in order to prevent hydrogen poisoning.

Conclusions

This paper provides evidence for competitive adsorption between nitrite and hydrogen during catalytic reduction of nitrite on Pd. Under steady state operation the system behaves according to the Langmuir-Hinshelwood model, showing negative reaction orders in hydrogen in case of low concentrations of nitrite. Transient operation of the membrane reactor confirmed this competitive adsorption via two observations; first, H_2 induces desorption of NO_2^- and second, the consumption of NO_2^- via adsorption and conversion on a catalyst saturated with hydrogen is enhanced when the coverage of the catalyst with hydrogen decreases during the experiment. Ammonia production via hydrogenation of the N-containing species on the catalyst surface proceeds via a fast and a slow pathway, both producing about equal amounts of ammonia. The slow path is attributed to unreactive atomic N species adsorbed on the Pd surface, which are kinetically irrelevant under steady state conditions.

Experimental Section

Materials Used

Macro porous alumina (α-Al_2O_3) tubes, length 200 mm, inner and outer diameter 0.9 and 1.9 mm respectively, were purchased from Hyflux CEPAration Technologies, Europe. They are cut to pieces of approximately 55 mm in length to serve as support for the carbon

nanofibers. Nickel nitrate hexahydrate (Merck), urea (Merck) and nitric acid (65%, Merck) were used to deposit nickel on the alumina tubes. Ethylene (99.95% PRAXAIR), hydrogen and nitrogen (99.999% INDUGAS) were used to grow CNFs without any further purification. Palladium acetylacetonate (Alfa Aesar) and toluene (> 99.9%, Merck) were used to deposit palladium. Toluene (>99.9% Merck) and a two component PDMS RTV 615 kit (permacol B.V.) consisting of a vinyl terminated pre-polymer (RTV–A) and a Pt-catalyzed cross-linker (RTV-B) were used for the preparation of the PDMS solution. Sodium nitrite (>99%, Merck) was used as nitrite source for the catalytic tests.

Reactor Preparation

The synthesis of the used membrane reactor is described in detail in [28]. In summary, deposition-precipitation technique was used to load nickel on the alumina tubes. Nickel was reduced and sintered at 850 °C in a hydrogen/nitrogen mixture (50/50) for 2 h. The temperature was decreased to 600 °C under inert atmosphere (nitrogen), followed by CNF growth in a quartz tube reactor of 10 mm diameter at 600 °C using a gas mixture containing 20% ethylene, 7% H_2, and 73% N_2. Next, the temperature was cooled to room temperature under 80 ml/min of nitrogen gas.

Sonication in milliQ water was used to remove any loose carbon nanofiber strands. After drying the sample, palladium was deposited using palladium acetylacetonate as precursor and calcined and reduced at 250 °C. The outer wall of the alumina tube was coated with a home-made PDMS membrane.

Catalytic Test

Two sets of experiments were performed, i.e. steady state experiments and experiments in transient operation. The experiments and results of steady state operation have already in part been reported earlier in [28] and are repeated here for clarity reasons.

In steady state experiments, a nitrite solution (44 μmol/L NO_2^-) saturated with argon was flowed inside the tube at a flowrate of 0.05 ml/min, while the shell of the membrane reactor was exposed to a gas mixture containing between 0.02 and 1.0 bar of hydrogen, balanced with argon. The gas flowrate (typically 50 ml/min) was sufficient to prevent any change in the H_2 concentration in the shell caused by H_2 consumption. Hydrogen diffuses through the PDMS membrane and meets the nitrite to react at the palladium particles located on the carbon nanofibers. All experiments were performed at room temperature (20 °C). Nitrite and ammonia concentrations were measured at the inlet and outlet of the membrane reactor with an in-line Ion Chromatograph (IC, Dionex, ICS 1000). Nitrite conversion and ammonia selectivity were calculated based on these concentrations using Equations (1) and (2). The solutions were not buffered. Selectivity to N_2 was calculated based on the molar balance and the fact that NH_4^+ and N_2 are the only products under used conditions.[18,29,37]

$$NO_2^- \text{ conversion} = \frac{[NO_2^-]_{in} - [NO_2^-]_{out}}{[NO_2^-]_{in}} \cdot 100\,\% \quad (1)$$

$$NH_4^+ \text{ selectivity} = \frac{[NH_4^+]_{out} - [NH_4^+]_{in}}{[NO_2^-]_{in} - [NO_2^-]_{out}} \cdot 100\,\% \quad (2)$$

Transient experiments were performed under similar conditions as described above, with the important difference that hydrogen and nitrite were fed to the reactor separated in time. The catalyst was first saturated overnight with hydrogen (1 bar continuous flow from the shell side). The shell side was flushed with argon for 10 minutes at 50 ml/min, after which all gas flows to the shell side are stopped, leaving a stagnant volume of argon in the shell. Next, the nitrite solution was fed to the inside of the tube, recording nitrite as well as ammonia concentrations in the ingoing and outgoing aqueous solution. The experiment continued until the moment that no conversion of nitrite was detected anymore, due to the exhaustion of the adsorbed hydrogen. At that point in time, the reverse experiment was started by flowing milliQ water (saturated with Ar) inside the membrane tube and flushing the shell with 1 bar H_2 at 50 ml/min. The experiment was continued until neither ammonia, nor nitrite was detectable anymore in the exit stream.

Characterization

The characterization of the membrane reactor is described in detail in [28], and is summarized in Table 1. All experiments were performed with a reactor with a homogeneous distribution of CNFs and Pd through the α-alumina tube.

Table 1. Characterization of the membrane reactor.

CNF growth time [min]	45
Carbon percentage [wt.%]	8.5
Total CNF pore filling [vol%] (Hg porosimetry)	29
CNF pore filling in carbon region [vol%]	29
Surface area [m^2/g reactor] (N_2 physisorption)	22.0
Pd loading [gPd/100 g reactor] (XRF)	0.077
Pd particle size [nm] (HR-SEM)	8–9

Acknowledgements

This work is supported by NanoNextNL, a micro and nanotechnology consortium of the Government of The Netherlands and 130 partners. We are thankful to K. Altena – Schildkamp and T.M.L Velthuizen for chemical analysis and D. Rafieian for help with the membrane-reactor synthesis.

Conflict of Interest

The authors declare no conflict of interest.

Keywords: nitrite · hydrogenation · competitive adsorption · membrane reactor · carbon nanofiber

[1] G. J. A. Speijers, J.K Fawell, *Nitrate and nitrite in drinking-water*, WHO publications, Geneva, **2011**.
[2] D. B. Kim-Shapiro, M. T. Gladwin, R. P. Patel, N. Hogg, *J. Inorg. Biochem.* **2005**, *99*, 237–246.
[3] A. A. Avery, *Environ. Health Perspect.* **1999**, *107*, 583–586.
[4] T. M. Addiscott, N. Benjamin, *Soil Use Manage.* **2004**, *20*, 98–104.
[5] European Commission, *concerning the protection of waters against pollution caused by nitrates from agricultural sources based on Member State reports for the period 2008–2011*, Brussels, **2013**.
[6] Environmental Protection Agency, *Nitrates and Nitrites*, in: E. P. Agency (Ed.), **2007**.

[7] Drinking Water and Groundwater Bureau, *Nitrate and Nitrite in Drinking Water*, in: Environmental Services (Ed.), Drinking Water and Groundwater Bureau, New Hampshire, **2010**.
[8] Archna, U. K. Sharma, R. C. Sobti, *E-J. Chem.* **2011**, *9*, 1667–1675.
[9] A. Kapoor, T. Viraraghavan, *J. Environ. Sci.* **1997**, *123*, 371–380.
[10] U. Prüsse, K.-D. Vorlop, *J. Mol. Catal. A* **2001**, *173*, 313–328.
[11] O. S. G. P. Soares, J. J. M. Órfão, M. F. R. Pereira, *Catal. Lett.* **2008**, *126*, 253–260.
[12] Y. Sakamoto, Y. Kamiya, T. Okuhara, *J. Mol. Catal. A* **2006**, *250*, 80–86.
[13] B. P. Chaplin, M. Reinhard, W. F. Schneider, C. Schüth, J. R. Shapley, T. J. Strathmann, C. J. Werth, *Environ. Sci. Technol.* **2012**, 46, 3655–3670.
[14] M. Hu, Y. Liu, Z. Yao, L. Ma, X. Wang, *Front. Environ. Sci. Eng.* **2018**, *12*, 3
[15] J. Martínez, A. Ortiz, I. Ortiz, *Appl. Catal. B* **2017**, *207*, 42–59
[16] K. Daub, G. Emig, M. J. Chollier, M. Callant, R. Dittmeyer, *Chem. Eng. Sci.* **1999**, *54*, 1577–1582.
[17] S. Hörold, T. Tacke, K. D. Vorlop, *Environ. Technol.* **1993**, *14*, 931–939.
[18] S. Hörold, K.-D. Vorlop, T. Tacke, M. Sell, *Chem. Informationsdienst* **1993**, *17*, 21–30.
[19] H. C. Aran, J. K. Chinthaginjala, R. Groote, T. Roelofs, L. Lefferts, M. Wessling, R. G. H. Lammertink, *Chem. Eng. J.* **2011**, *169*, 239–246.
[20] H. C. Aran, S. P. Benito, M. W. J. Luiten-Olieman, S. Er, M. Wessling, L. Lefferts, N. E. Benes, R. G. H. Lammertink, *J. Membr. Sci.* **2011**, *381*, 244–250.
[21] G. Strukul, R. Gavagnin, F. Pinna, E. Modaferri, S. Perathoner, G. Centi, M. Marella, M. Tomaselli, *Catal. Today* **2000**, *55*, 139–149.
[22] O. M. Ilinitch, F. P. Cuperus, L. V. Nosova, E. N. Gribov, *Catal. Today* **2000**, *56*, 137–145.
[23] K. Lüdtke, K.-V. Peinemann, V. Kasche, R.-D. Behling, *J. Membr. Sci.* **1998**, *151*, 3–11.
[24] H. C. Aran, H. Klooster, J. M. Jani, M. Wessling, L. Lefferts, R. G. H. Lammertink, *Chem. Eng. J.* **2012**, *207–208*, 814–821.
[25] H. C. Aran, J. K. Chinthaginjala, R. Groote, T. Roelofs, L. Lefferts, M. Wessling, R. G. H. Lammertink, *Chem. Eng. J.* **2011**, *169*, 239–246.
[26] N. Diban, A. T. Aguayo, J. Bilbao, A. Urtiaga, I. Ortiz, *Ind. Eng. Chem. Res.* **2013**, *52*, 10342–10354.
[27] R. Brunet Espinosa, D. Rafieian, R. G. H. Lammertink, L. Lefferts, *Catal. Today* **2016**, *273*, 50–61.
[28] R. Brunet Espinosa, D. Rafieian, R. S. Postma, R. G. H. Lammertink, L. Lefferts, *Appl. Catal. B* **2018**, *224*, 276–282.
[29] J. K. Chinthaginjala, L. Lefferts, *Appl. Catal. B* **2010** *101*, 144–149.
[30] Y. Matatov-Meytal, Y. Shindler, M. Sheintuch, *Appl. Catal. B* **2003**, *45*, 127–134.
[31] I. Mikami, Y. Sakamoto, Y. Yoshinaga, O. Okuhara, *Appl. Catal. B* **2003** *44*, 79–86.
[32] F. A. Lewis, *Platinum Met. Rev.* **1960**, *4*, 132–137.
[33] F. A. Lewis, *Platinum Met. Rev.* **1982**, *26*, 20–27.
[34] S. D. Ebbesen, B. L. Mojet, L. Lefferts, *J. Catal.* **2008**, *256*, 15–23.
[35] S. D. Ebbesen, B. L. Mojet, L. Lefferts, *J. Phys. Chem.* **2011**, *115*, 1186–1194.
[36] Y. Zhao, N. K. Rao, L. Lefferts, *J. Catal.* **2016**, *337*, 102–110.
[37] C. Francha, R. G. H. Lammertink, L. Lefferts, *Appl. Catal. B* **2014**, 156–157, 166–172.

Manuscript received: March 28, 2018
Accepted Article published: June 15, 2018
Version of record online: July 5, 2018